



Theoretical study of the magnetic and magnetocaloric properties of $\text{La}_{0.7}\text{Sr}_{0.3}\text{Mn}_{0.95}\text{Fe}_{0.05}\text{O}_3$ perovskite manganites at low and high applied magnetic fields: Landau theory and phenomenological models

ASME BRAHIMI^{1,2}, ABDELKRIM ELHASNAÏNE MERAD^{2,*} , MOHAMED ELLOUZE³ and MOHAMMED BENALI KANOUN⁴

¹Automatic Laboratory, A. Belkaid University, Box 119, 13000 Tlemcen, Algeria

²Solid State Physics Team, Theoretical Physics Laboratory, Faculty of Sciences, A. Belkaid University, Box 119, 13000 Tlemcen, Algeria

³Faculty of Sciences of Sfax, LMEEM, Sfax University, B.P. 1171, 3000 Sfax, Tunisia

⁴Department of Physics, College of Science, King Faisal University, P.O. Box 400, Al-Ahsa 31982, Saudi Arabia

*Author for correspondence (aemerad@gmail.com)

MS received 29 October 2021; accepted 17 January 2022

Abstract. In this study, the magnetic and magnetocaloric properties of a recently elaborated $\text{La}_{0.7}\text{Sr}_{0.3}\text{Mn}_{0.95}\text{Fe}_{0.05}\text{O}_3$ perovskite manganites have been modelled using different theoretical methods based on Landau theory and phenomenological models. The calculations were done by exploring the measurement data of magnetization vs. temperature at various low and high magnetic field values. The results confirmed that this compound has a magnetic phase transition of the second-order type from ferromagnetic to paramagnetic states at Curie temperature near the room temperature. The theoretical values of the magnetic entropy change ($-\Delta S_M$) are estimated in low and high applied magnetic fields from these methods. The analysis of our obtained results of the relative cooling power indicated that this compound is a potential candidate material for magnetic refrigeration technology.

Keywords. Perovskite manganites; magnetocaloric effect; Landau theory; phenomenological models.

1. Introduction

Due to global warming, the need to use cooling technologies, in particular, has increased. At the same time, the existing cooling systems consume 15% of electricity generated globally and account for 10% of global greenhouse gas emissions. Therefore, the demand for cooling is expected to grow tenfold by 2050 [1], which also puts huge pressure on the electrical systems in many countries, while rising emissions. However, alternative coolers must be found or developed. Among the potential cooling technologies, magnetic refrigeration can be considered as a new emerging and alternative technology to conventional gas compression refrigeration systems. This emergent technology does not require the use of ozone-depleting or greenhouse effect related gases, which makes it environmentally friendly [2], large refrigeration efficiency and energy saving [3]. Magnetic refrigeration is based on the magnetocaloric effect (MCE) property of magnetic materials. The MCE is defined by a heating or cooling of a magnetic material under a change of a magnetic field.

It is known that the MCE is characterized by an adiabatic temperature change (ΔT_{ad}) and isothermal magnetic

entropy change (ΔS_M), induced by a variation of the external magnetic field [4]. Therefore, the MCE should exhibit the highest values near the magnetic phase transition temperature of the materials. In this context, the gadolinium (Gd) metal has been considered as the most active magnetic refrigerant at room temperature magnetic refrigerators with a large MCE, but its exorbitant price tag, which could be as high as \$ 4,000 kg⁻¹, made its use somewhat limited [5]. Consequently, a lot of research has been done on magnetic materials that offered the best magnetic properties at a lower price, yielding many magnetocaloric materials. The rare-earth manganite perovskite with the general formula $(R_{1-x}^{3+}A_x^{2+})(Mn_{1-x}^{3+}Mn_x^{4+})O_3^{2-}$ ($R = \text{La, Nd, ...}$ $A = \text{Co, Sr, Ba, ...}$) has been the subject of a large number of recent studies due to their large range of properties such as colossal magnetoresistance (CMR) and MCE [6]. These materials may be industrially preferable because they offer several advantages: low production cost, chemical stability, corrosion-free effect and high resistivity [7]. Among the various manganite perovskites, $\text{La}_{0.7}\text{Sr}_{0.3}\text{MnO}_3$ is ferromagnetic with a transition at the highest value of Curie temperature $T_c = 360 \text{ K}$ [8]. It is distinguished by a

maximum change of magnetic entropy (ΔS_M^{\max}) corresponding to $2.68 \text{ J kg}^{-1} \text{ K}^{-1}$ under a magnetic field of $2T$ at 370 K , which is advantageous for technological applications. To further improve the MCE properties of manganite perovskite, the new investigation strategy is advanced by the prospects of realizing new systems, by means of substituting rare earth with a divalent ion as Sr^{2+} to obtain a large range of magnetic entropy change. Moreover, the Mn-site substitutions with transition metal as Fe [9] can also be applied to control magnetic entropy change owing to the weakened double-exchange interactions between Mn^{3+} and Mn^{4+} ions of the pristine structures.

Many experimental works based on $\text{La}_{0.7}\text{Sr}_{0.3}\text{MnO}_3$ materials, with tailoring the MCE properties through divalent and transition metals dopants, have been achieved. More recently, Dhahri and co-workers [10] have investigated the experimental synthesis of $\text{La}_{0.7}\text{Sr}_{0.3}\text{Mn}_{0.95}\text{Fe}_{0.05}\text{O}_3$ by using solid-state reaction technique. They reported that doping 5% of Fe at Mn sites in $\text{La}_{0.7}\text{Sr}_{0.3}\text{MnO}_3$ can lead to a transition from ferromagnetic to paramagnetic state with increasing temperature. Here, a Curie temperature of 310 K was observed. Several theoretical methods are performed to study the MCE such as phenomenological and statistical approaches. These methods are based fundamentally on the temperature dependence of the magnetization ($M(T)$) data [11–13]. However, the results depend essentially on the choice of the used method, the temperature interval and the applied magnetic field intensity.

Motivated by the experimental progress of the MCE towards the doping of Fe with Mn, we used different theoretical methods based on Landau's theory and phenomenological models such as those of Hamad [14], Franco *et al* [15] and Maxwell relations, in order to simulate the dependence of the magnetization on the temperature change and hence, to determine the magnetocaloric properties, including the change of magnetic entropy, change in heat capacity and relative cooling power (RCP) for low and high applied magnetic fields.

2. Methodology

As indicated above, the chosen material, namely the perovskite manganite $\text{La}_{0.7}\text{Sr}_{0.3}\text{Mn}_{0.95}\text{Fe}_{0.05}\text{O}_3$ was recently elaborated by solid-state reaction at higher temperature up to 1400°C , using several oxide precursors La_2O_3 , SrCO_3 , MnO_2 and Fe_2O_3 in the form of powders. The structural, magnetic magnetocaloric properties as well as the critical exponents were investigated. RCP is obtained for an applied magnetic field of 5 T . More details are given in [10]. We explored the experimental data of the magnetization *vs.* temperature $M_{-\mu_0 H}$ for several applied magnetic fields. Among the main goals of our theoretical study is to analyse the behaviour of the RCP and provide the corresponding

values for a wide range of the applied magnetic fields (low and high), since the only available experimental value is given only for 5 T .

For that, two theoretical methods are used: The first method that we have chosen for high magnetic fields is the basic computational Landau theory. It is coupled with the 'soft mode' concept, which provides a simple picture of many structural phase transitions in terms of relatively few phenomenological constants [16]. The second method is the model of Hamad that we have chosen for low magnetic fields. It has been widely used in recent years to investigate the magnetocaloric properties for a magnetic system, and which had previously shown its efficiency, for low applied magnetic fields, for example, in $\text{Nd}_{0.67}\text{Ba}_{0.33}\text{MnO}_3$ and $\text{Pr}_{0.5}\text{Sr}_{0.5}\text{MnO}_3$ manganites [17,18]. Our results of the magnetocaloric effect obtained by these two above methods were compared and consolidated with our results obtained using the Maxwell relation.

Finally, we extended our study to evaluate the universal curve of the magnetic entropy $\Delta S_M(T)$ for the $\text{La}_{0.7}\text{Sr}_{0.3}\text{Mn}_{0.95}\text{Fe}_{0.05}\text{O}_3$, below and above T_c , using the Franco *et al* [15] universal model. We predicted the corresponding free parameter values related to this compound. More details on these theoretical considerations of our methodology regarding the Landau theory and several models as indicated above, are described in the following.

2.1 Landau theory of phase transitions

The main idea of the Landau theory, in its original general form, is simply that out of all the complexities of statistical mechanics, one can (e.g., mean-field theory) reduce the behaviour of a system undergoing a phase transformation to that of a few order parameters governed by a free energy functional, which depends on those order parameters, temperatures and pressure [19]. According to this theory, Amaral *et al* [20,21] proposed a model with a contribution from the magnetoelastic and electronic interaction in manganites, where free energy is dependent on three coefficients $A(T)$, $B(T)$ and $C(T)$. Recently, in order to reduce the difference between the experimental results and the results of this model [22], Hsini *et al* [23] added another coefficient $D(T)$, and the development of the free energy as a function of the temperature T and the magnetization M will be in the eighth order as follows:

$$G(T, M) \cong G_0 + \frac{1}{2}A(T)M^2 + \frac{1}{4}B(T)M^4 + \frac{1}{6}C(T)M^6 + \frac{1}{8}D(T)M^8 - \mu_0 HM. \quad (1)$$

Equation (1) is minimized with respect to the magnetization M ($\frac{\partial G}{\partial M} = 0$). After this step, the magnetic equation of state is:

$$\frac{H}{M} = A(T) + B(T)M^2 + C(T)M^4 + D(T)M^6. \quad (2)$$

The parameters $A(T)$, $B(T)$, $C(T)$ and $D(T)$ represent the Landau coefficients. The magnetic entropy change is obtained from the differentiation of the magnetic part of the free energy with respect to temperature as follows:

$$\begin{aligned} S(T, M) &= \left(\frac{\partial G(\mu_0 H, T)}{\partial T} \right)_H \\ &\cong \frac{1}{2} A'(T) M^2 + \frac{1}{4} B'(T) M^4 + \frac{1}{6} C'(T) M^6 \\ &\quad + \frac{1}{8} D'(T) M^8 \end{aligned} \quad (3)$$

where $A'(T) = \frac{\partial A}{\partial T}$, $B'(T) = \frac{\partial B}{\partial T}$, $C'(T) = \frac{\partial C}{\partial T}$ and $D'(T) = \frac{\partial D}{\partial T}$.

Based on the renormalization group approach to scaling [24], Dong *et al* [25] have reported that the variation of entropy under a zero magnetic field is not zero. So, it is written as follows:

$$\begin{aligned} -\Delta S_M(T, \mu_0 H) &= S_M(T, \mu_0 H) - S_M(T, 0) \\ &= \frac{1}{2} A'(T) (M^2 - M(0)^2) + \frac{1}{4} B'(T) (M^4 - M(0)^4) \\ &\quad + \frac{1}{6} C'(T) (M^6 - M(0)^6) + \frac{1}{8} D'(T) (M^8 - M(0)^8). \end{aligned} \quad (4)$$

RCP is given as [26]:

$$\text{RCP} = -\Delta S_M^{\text{max}}(T, \mu_0 H_{\text{max}}) \times \delta T_{\text{FWHM}}. \quad (5)$$

2.2 Phenomenological model of Hamad

According to the phenomenological model of Hamad [14], the variation of the magnetization as a function of temperature for an applied magnetic field is modelled by the following relation:

$$M = \left(\frac{M_i - M_f}{2} \right) \tanh(A(T_c - T)) + BT + C \quad (6)$$

where M_i and M_f represent respectively the initial and the final values of the magnetization at the ferromagnetic-paramagnetic transition (FM-PM). T_c is the Curie temperature at which $\left(\frac{dM}{dT} \right)$ shows a minimum. The coefficients A , B and C are defined as:

$$\begin{cases} A = \frac{2(B - S_c)}{M_i - M_f}, \\ B = \left(\frac{dM}{dT} \right)_{T_i}, \\ C = \left(\frac{M_i + M_f}{2} \right) - BT_c, \end{cases}$$

where $S_c = \left(\frac{dM}{dT} \right)_{T_c}$. The variation of magnetic entropy under a variation $\Delta\mu_0 H$ magnetic field can be calculated by

equation (7), and the maximum of this variation obtained at $T = T_c$ can be calculated by equation (8). Thus

$$\begin{aligned} \Delta S_M &= \int_0^{\mu_0 H_{\text{max}}} \left(\frac{\partial M}{\partial T} \right)_H d\mu_0 H \\ &= \left(-A \left(\frac{M_i - M_f}{2} \right) \text{sech}^2(A(T_c - T)) + B \right) \mu_0 H_{\text{max}}, \end{aligned} \quad (7)$$

$$\Delta S_{\text{max}} = \mu_0 H_{\text{max}} \left(-A \left(\frac{M_i - M_f}{2} \right) + B \right). \quad (8)$$

The full-width at half-maximum δT_{FWHM} can be evaluated by the following equation:

$$\delta T_{\text{FWHM}} = \frac{2}{A} \cos^{-1} \left(\sqrt{\frac{2A(M_i - M_f)}{A(M_i - M_f) + 2B}} \right). \quad (9)$$

RCP, according to the phenomenological model is given by

$$\begin{aligned} \text{RCP} &= -\Delta S_M(T, \mu_0 H_{\text{max}}) \times \delta T_{\text{FWHM}} \\ &= \left(M_i - M_f - 2 \frac{B}{A} \right) \mu_0 H_{\text{max}} \\ &\quad \times \cos^{-1} \left(\sqrt{\frac{2A(M_i - M_f)}{A(M_i - M_f) + 2B}} \right). \end{aligned} \quad (10)$$

The values of the heat capacity change are given by:

$$\begin{aligned} \Delta C_{P,H} &= -TA^2(M_i - M_f) \text{sech}^2(A(T_c - T)) \\ &\quad \tanh(A(T_c - T)) \mu_0 H_{\text{max}}. \end{aligned} \quad (11)$$

2.3 Maxwell relation

The magnetic entropy is related to the magnetization M , the magnetic field strength $\mu_0 H$ and the absolute temperature T through the following Maxwell relation [27]:

$$\left(\frac{\partial S}{\partial \mu_0 H} \right)_T = \left(\frac{\partial M}{\partial T} \right)_{\mu_0 H}, \quad (12)$$

which means that

$$\begin{aligned} \Delta S_M(T, \Delta\mu_0 H) &= S_M(T, \mu_0 H) - S_M(T, 0) \\ &= \int_0^{\mu_0 H} \left(\frac{\partial M}{\partial T} \right)_{\mu_0 H} d\mu_0 H. \end{aligned} \quad (13)$$

The numerical integration of the latter gives the values of ΔS_M in terms of M_{i+1} and M_i being the magnetization values measured at T_{i+1} and T_i temperatures at different values of fields according to the following equation [28]:

$$\Delta S_M(T, \Delta\mu_0 H) = \sum \frac{M_i - M_{i+1}}{T_i - T_{i+1}} d\mu_0 H. \quad (14)$$

The efficiency of materials in the magnetocaloric application as a function of the change in magnetic entropy defined by a parameter called RCP, is given as [26]:

$$\text{RCP} = -\Delta S_M^{\text{max}}(T, \mu_0 H_{\text{max}}) \times \delta T_{\text{FWHM}}, \quad (15)$$

where δT_{FWHM} is the full-width at half-maximum of the magnetic entropy change curve.

2.4 Phenomenological universal model of Franco *et al*

In last decade, a phenomenological universal curve for the temperature dependence of ΔS_M measured at different fields has been proposed by Franco *et al* [15]. According to this model, in the case of a second-order phase transition, all $\Delta S_M(T)$ curves are normalized with their respective peak entropy change ΔS_M^{max} , as $\Delta S' = \Delta S_M(T)/\Delta S_M^{\text{max}}$. For the temperature axis, it should be rescaled in a different way, below and above T_c , as follows:

$$\theta = \begin{cases} \frac{T_c - T}{T_{r1} - T_c}, & T \leq T_c \\ \frac{T - T_c}{T_{r2} - T_c}, & T > T_c \end{cases} \quad (16)$$

θ represents the rescaled temperature, T_{r1} and T_{r2} are the temperatures of the two reference points corresponding to $\Delta S_M(T_{r1,2}) = \Delta S_M^{\text{max}}/2$. The universal curve can be well-fitted by a Lorentz function [29]

$$\Delta S' = \frac{a}{b + (\theta - c)^2}, \quad (17)$$

where a , b and c are the free parameters.

3. Results and discussion

To identify the nature of the magnetic phase transition of $\text{La}_{0.7}\text{Sr}_{0.3}\text{Mn}_{0.95}\text{Fe}_{0.05}\text{O}_3$, the isothermal magnetization values are gathered near T_c . Figure 1 depicts the plots of Arrott (H/M vs. M^2). All plotted curves illustrate positive slopes, indicating a second-order magnetic transition of

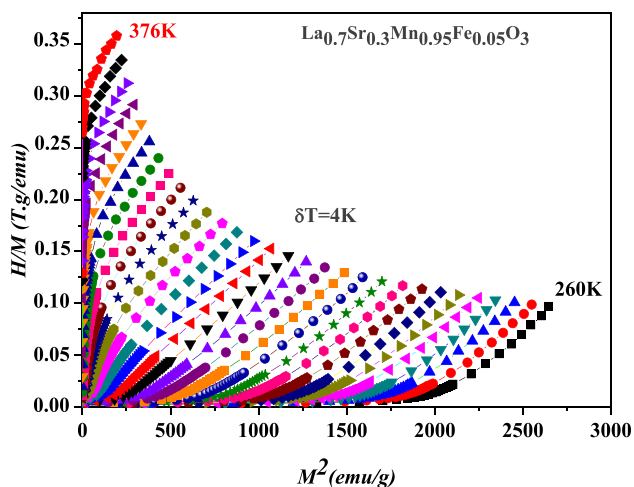


Figure 1. Arrott plot curves (cubic fits) of H/M vs. M^2 .

$\text{La}_{0.7}\text{Sr}_{0.3}\text{Mn}_{0.95}\text{Fe}_{0.05}\text{O}_3$. Arrott diagrams are also designated to determine Landau coefficients using a series of cubic adjustments that was applied to the plots.

The temperature dependence of the Landau coefficients $A(T)$, $B(T)$, $C(T)$ and $D(T)$ obtained for the compound $\text{La}_{0.7}\text{Sr}_{0.3}\text{Mn}_{0.95}\text{Fe}_{0.05}\text{O}_3$ is shown in figure 2. The results showed that values of A change from negative, the value of characteristic temperature T_c corresponding to the minimum positive value, knowing that the sign of coefficient B at this point is obtained. According to the Banerjee criterion [30], the investigated system $\text{La}_{0.7}\text{Sr}_{0.3}\text{Mn}_{0.95}\text{Fe}_{0.05}\text{O}_3$ has a second-order FM–PM transition. For the other coefficients, when $T > T_c$, $C(T)$ decreases and $D(T)$ increases.

The entropy variation $-\Delta S_M(T, \mu_0 H)$ under different values of the high magnetic field are estimated. The entropy changes as a function of temperature under 1T, 2T, 3T, 4T and 5T are illustrated in figure 3 compared with our estimated values from experimental data [10], using the Maxwell relation. We found that our results obtained by Landau theory are in good qualitative and quantitative agreement with the experimental data [10]. Table 1 summarizes magnetocaloric properties for $\text{La}_{0.7}\text{Sr}_{0.3}\text{Mn}_{0.95}\text{Fe}_{0.05}\text{O}_3$, obtained from Landau theory and Maxwell relation for several magnetic field (1 to 5) T. The inset of figure 3 shows the proportional relationship between the applied magnetic field ($\mu_0 H$) and the magnetocaloric properties. In fact, when the magnetic field strength ($\mu_0 H$) increases, the maximum of the entropy change $|\Delta S_M^{\text{max}}|$ increases, giving rise to an increase in the magnetocaloric properties through the RCP quantity. Compared to the results of other candidate materials shown in table 2, $\text{La}_{0.7}\text{Sr}_{0.3}\text{Mn}_{0.95}\text{Fe}_{0.05}\text{O}_3$ is found to be a better material for magnetic refrigeration application at room temperature region.

The magnetic field dependence of $|\Delta S_M^{\text{max}}|$ can be expressed as a power law of the magnetic field given by [31]:

$$|\Delta S_M^{\text{max}}| \approx a(\mu_0 H)^n, \quad (18)$$

where a is a constant and the exponent n depends on the magnetic state of the sample [32]. We have determined these two parameters by fitting equation (18) to our results obtained by Landau theory. The corresponding behaviour is illustrated in figure 4a and the values of constants a and n are found to be 0.555 and 0.862 at T_c , respectively. Similarly, to the field dependence of ΔS_M^{max} , the RCP also followed the same nature of power law with the magnetic field, given by equation (19) [33] as:

$$\text{RCP} \approx b(\mu_0 H)^m, \quad (19)$$

where b and m are constant parameters.

Figure 4b illustrates the variation of the RCP as a function of the magnetic field $\mu_0 H$ based on the fitting of our results from Landau theory, using equation (19). The obtained parameters are given as $b = 19.07$ and $m = 1.173$.

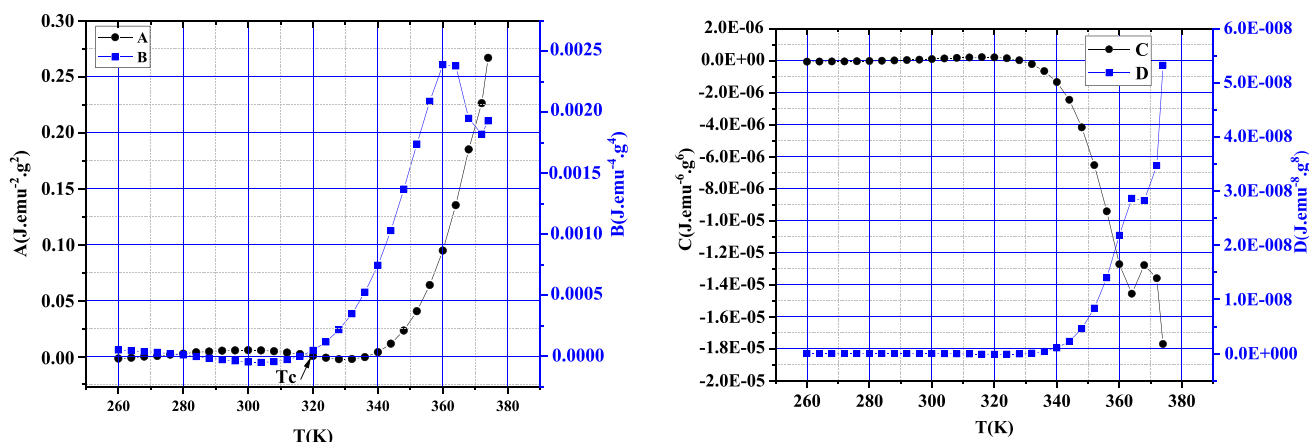


Figure 2. Variation of the Landau coefficients $A(T)$, $B(T)$, $C(T)$ and $D(T)$ vs. temperature.

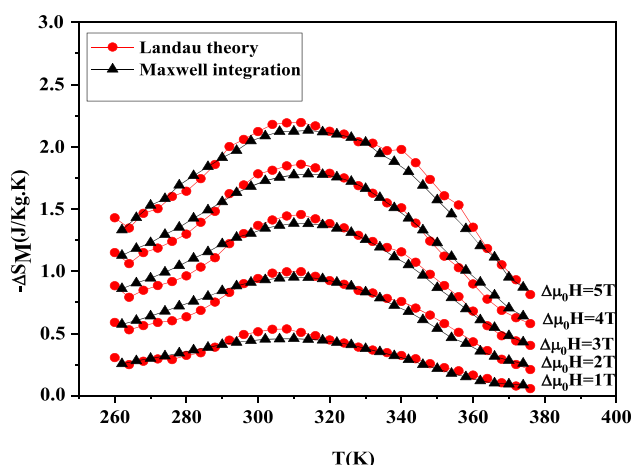


Figure 3. $-\Delta S_M(T, \mu_0 H)$ vs. temperature under magnetic field applied. The red symbols represent modelled results (using equation (4)) and black symbols represent Maxwell results from experimental data [10].

At this step we showed that our results obtained with the Landau theory gives good prediction of the magnetocaloric properties of $\text{La}_{0.7}\text{Sr}_{0.3}\text{Mn}_{0.95}\text{Fe}_{0.05}\text{O}_3$ for high applied magnetic field, compared to the results reported in [10]. Therefore, it is interesting to examine and evaluate the properties for low applied magnetic field by using a phenomenological model of Hamad [14]. However, the results for low magnetic fields are not available, and for that, we also used the Maxwell’s relation to consolidate our final results.

First of all, using experimental data for low magnetic fields, we extracted the parameters mentioned previously (M_i, M_f, T_c, B, S_c), and the obtained values are given in table 3. Using these parameters and by applying equation (10), we calculate the temperature dependence of the magnetization for $\text{La}_{0.7}\text{Sr}_{0.3}\text{Mn}_{0.95}\text{Fe}_{0.05}\text{O}_3$ at several values of applied magnetic field, as shown in figure 5. The obtained magnetization agrees well with the experimental

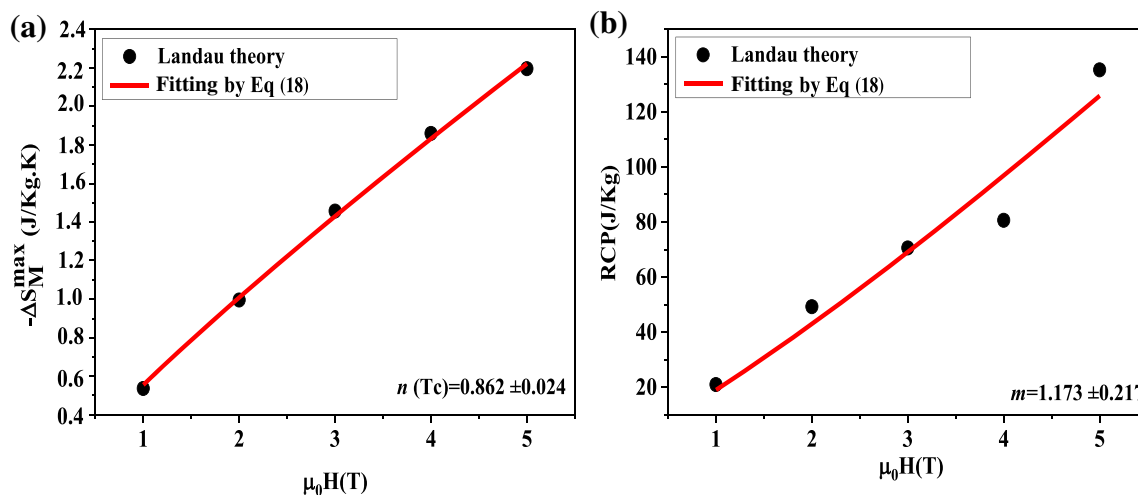
Table 1. Comparison between values of magnetocaloric properties for $\text{La}_{0.7}\text{Sr}_{0.3}\text{Mn}_{0.95}\text{Fe}_{0.05}\text{O}_3$ obtained from Landau theory and Maxwell relation.

Method	$\Delta\mu_0 H$ (T)	$-\Delta S_M^{\max}$ (J kg ⁻¹ K ⁻¹)	δT_{FWHM} (K)	RCP (J Kg ⁻¹)	Ref.
Landau theory	1	0.536	39.176	20.991	This study
	2	0.995	49.417	49.205	This study
	3	1.456	53.250	77.517	This study
	4	1.859	54.391	80.607	This study
	5	2.194	61.617	135.218	This study
Maxwell relation	1	0.45813	52.285	23.953	This study
	2	0.95116	52.699	50.125	This study
	3	1.3839	54.359	75.227	This study
	4	1.7807	56.849	101.231	This study
	5	2.132	63.903	136.241	This study
	5	2.13	—	127.9	[10] ^(a)

^(a)Obtained from the experimental data.

Table 2. Estimated values of magnetocaloric properties for $\text{La}_{0.7}\text{Sr}_{0.3}\text{Mn}_{0.95}\text{Fe}_{0.05}\text{O}_3$ from Landau theory compared with those of other compounds.

Compound	$\Delta\mu_0 H$ (T)	$-\Delta S_M^{\max}$ (J kg ⁻¹ K ⁻¹)	RCP (J kg ⁻¹)	Ref.
$\text{La}_{0.7}\text{Sr}_{0.3}\text{Mn}_{0.95}\text{Fe}_{0.05}\text{O}_3$	5	2.194	135.218	This study
$\text{Ce}_{0.67}\text{Sr}_{0.33}\text{MnO}_3$	5	1.65	41.41	[34]
$\text{La}_{0.7}\text{Sr}_{0.3}\text{Mn}_{0.95}\text{Fe}_{0.05}\text{O}_3$	2	0.995	49.205	This study
$\text{Pr}_{0.6}\text{Sr}_{0.4}\text{MnO}_3$	2.5	2.3	34.5	[35]
$\text{La}_{0.7}\text{Sr}_{0.3}\text{MnO}_3$	2	1.27	29	[36]

**Figure 4.** (a) Magnetic entropy change $|\Delta S_M^{\max}|$ vs. $\mu_0 H(T)$; (b) RCP vs. $\mu_0 H(T)$ for $\text{La}_{0.7}\text{Sr}_{0.3}\text{Mn}_{0.95}\text{Fe}_{0.05}\text{O}_3$.

data. The $M(T)$ curves show that the sample $\text{La}_{0.7}\text{Sr}_{0.3}\text{Mn}_{0.95}\text{Fe}_{0.05}\text{O}_3$ has a magnetic transition from ferromagnetic to paramagnetic at T_c near the room temperature.

We determined the dependence of magnetic entropy changes with temperature using both Maxwell relation and phenomenological model of Hamad at different low magnetic fields: (0.1, 0.15, 0.2) T for $\text{La}_{0.7}\text{Sr}_{0.3}\text{Mn}_{0.95}\text{Fe}_{0.05}\text{O}_3$, as illustrated in figure 6. We can see that the magnetic entropy changes increases and reaches the maximum near the room temperature for two used methods.

Table 4 summarizes our calculated magnetocaloric properties of $\text{La}_{0.7}\text{Sr}_{0.3}\text{Mn}_{0.95}\text{Fe}_{0.05}\text{O}_3$ estimated with Maxwell relation and Hamad model for different values of low magnetic field.

The interesting step now is to present an analysis of the magnetic entropy changes ΔS_M using a phenomenological universal model proposed by Franco *et al* [15] as described above. All $\Delta S_M(T)$ curves are normalized with their respective peak entropy change ΔS_M^{\max} . The collapse of these curves, together with the rescaled ΔS_M of the curves is shown in figure 7. All these curves collapse into one universal curve, which confirms that the $\text{La}_{0.7}\text{Sr}_{0.3}\text{Mn}_{0.95}\text{Fe}_{0.05}\text{O}_3$ system presents a second-order phase transition. The universal curve is fitted by equation (17) of the Lorentz function, by taking into account the asymmetry of the curve. Our predicted free parameters corresponding to the universal curve for the $\text{La}_{0.7}\text{Sr}_{0.3}\text{Mn}_{0.95}\text{Fe}_{0.05}\text{O}_3$, below and above T_c are given as:

Table 3. Hamad model parameters for $\text{La}_{0.7}\text{Sr}_{0.3}\text{Mn}_{0.95}\text{Fe}_{0.05}\text{O}_3$ at low applied magnetic field values.

$\mu_0 H(T)$	M_i (emu g ⁻¹)	M_f (emu g ⁻¹)	T_c (K)	B (emu g ⁻¹ K ⁻¹)	S_c (emu g ⁻¹ K ⁻¹)
0.1	30.16	3.04	308	- 0.05	- 0.44
0.15	35.51	3.1	308	- 0.06	- 0.502
0.2	37.68	3.68	308	- 0.068	- 0.526

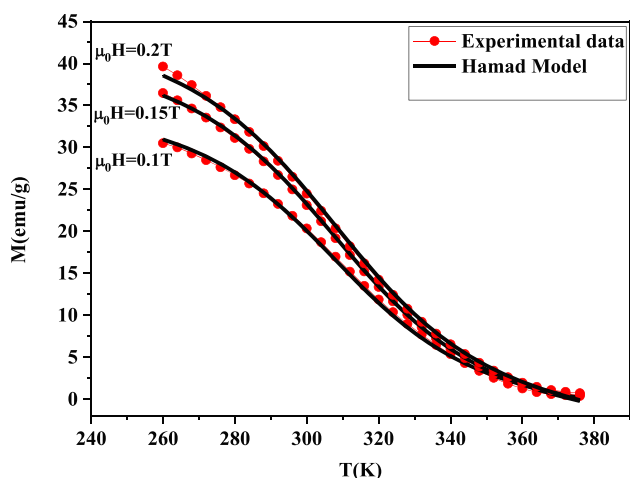


Figure 5. Magnetization vs. temperature under low magnetic field. The red lines represent modelled results and symbols represent the experimental data.

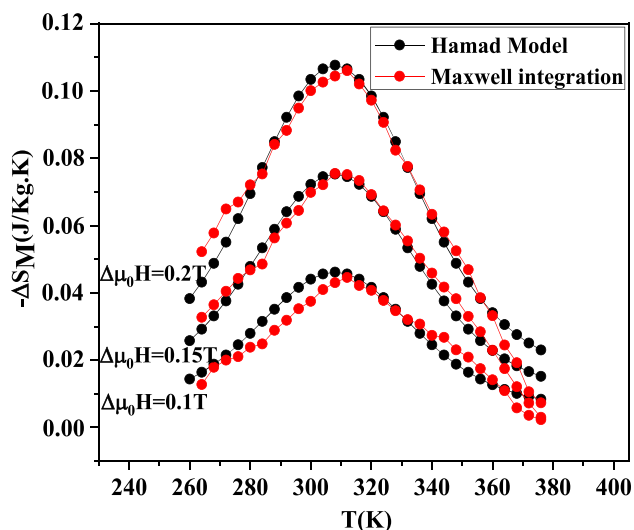


Figure 6. Calculated magnetic entropy changes of $\text{La}_{0.7}\text{Sr}_{0.3}\text{Mn}_{0.95}\text{Fe}_{0.05}\text{O}_3$ vs. temperature under a low magnetic field. The red symbols represent Maxwell integration results and the black symbols represent modelled results by Hamad model.

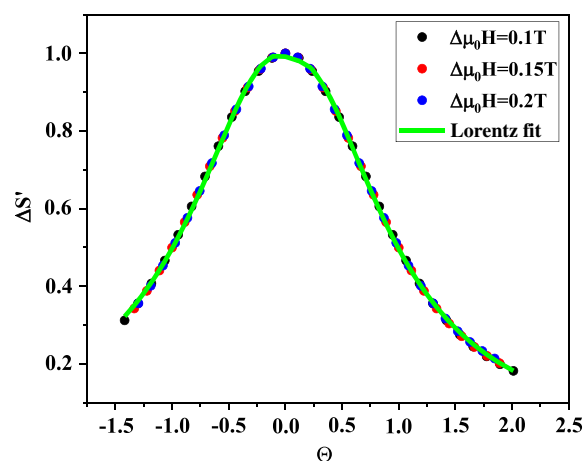


Figure 7. Universal behaviour of magnetic entropy curves for $\text{La}_{0.7}\text{Sr}_{0.3}\text{Mn}_{0.95}\text{Fe}_{0.05}\text{O}_3$ at low magnetic fields.

- For $T \leq T_c$: $a = 0.882$, $b = 0.885$ and $c = -0.058$.
- For $T > T_c$: $a = 0.821$, $b = 0.837$ and $c = 0.095$.

The variation of the heat capacity change ΔC_p with the temperature under low magnetic fields is shown in figure 8. It is calculated using equation (11) depending on the results of Hamad’s model of the magnetization change. The curve shows the change of ΔC_p from positive to negative around T_c . The sum of the two parts is the magnetic contribution to the total specific heat, which affects the cooling or heating power of the magnetic refrigerator or the adiabatic temperature change T_{ad} [37]. In addition, the estimated values of ΔC_p^{max} and ΔC_p^{min} are given in table 4 and are proportional to the applied magnetic field.

4. Conclusion

In conclusion, magnetic and magnetocaloric properties of $\text{La}_{0.7}\text{Sr}_{0.3}\text{Mn}_{0.95}\text{Fe}_{0.05}\text{O}_3$ perovskite were investigated theoretically using the Landau theory in addition to other phenomenological models. The calculations were done by exploring the measurement data of magnetization vs. temperature at various low and high magnetic field values. It

Table 4. Calculated values of magnetocaloric properties for $\text{La}_{0.7}\text{Sr}_{0.3}\text{Mn}_{0.95}\text{Fe}_{0.05}\text{O}_3$.

Methods	$\Delta\mu_0 H$ (T)	$-\Delta S_M^{max}$ ($\text{J kg}^{-1} \text{K}^{-1}$)	δT_{FWHM} (K)	RCP (J kg^{-1})	ΔC_p^{max} ($\text{J kg}^{-1} \text{K}^{-1}$)	ΔC_p^{min} ($\text{J kg}^{-1} \text{K}^{-1}$)
Maxwell relation	0.1	0.047	50.625	2.379	—	—
	0.15	0.075	46.060	3.455	—	—
	0.2	0.108	45.645	4.930	—	—
Hamad model	0.1	0.046	67.829	3.120	0.301	-0.257
	0.15	0.075	71.94	5.396	0.462	-0.395
	0.2	0.107	73.52	7.867	0.205	-0.552

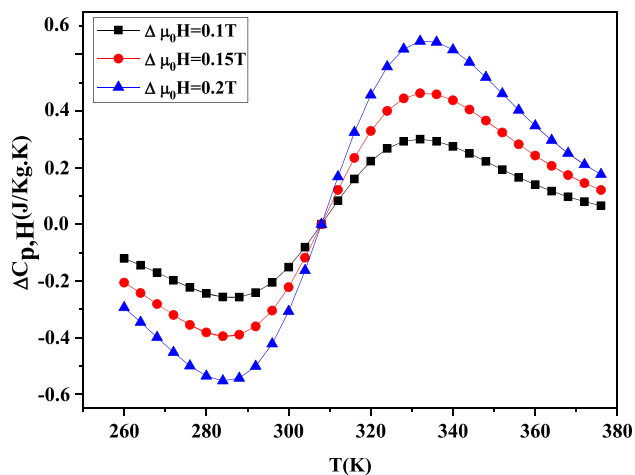


Figure 8. Heat capacity change of $\text{La}_{0.7}\text{Sr}_{0.3}\text{Mn}_{0.95}\text{Fe}_{0.05}\text{O}_3$ vs. temperature under low magnetic fields calculated by Hamad's model.

was observed that the magnetic phase transition from ferromagnetic to paramagnetic is of second order for which the Curie temperature is near the room temperature. The maximum of magnetic change reached significant values of 0.995 and $2.194 \text{ J kg}^{-1} \text{ K}^{-1}$ under a magnetic field of 2 and 5 T that accompanies a large full-width at half-maximum δT_{FWHM} . Consequently, RCP from Landau theory is deduced and compared with Maxwell relation, phenomenological models and experimental measurements. The obtained values of 135.2 J kg^{-1} (by Landau theory) and 136.2 J kg^{-1} (by Maxwell relation) are in good agreement with the only available experimental value of 127.9 J kg^{-1} evaluated at 5 T. These values indicate that $\text{La}_{0.7}\text{Sr}_{0.3}\text{Mn}_{0.95}\text{Fe}_{0.05}\text{O}_3$ compound is more suitable for non-polluting magnetic refrigeration technology.

Acknowledgements

AEM is grateful to DGRSDT and MHESR of Algeria for financial support under the PRFU research project No. B00L02UN130120180011.

References

- [1] Goldstein E A, Raman A P and Fan S 2017 *Nat. Energy* **2** 1
- [2] Franco V, Blázquez J S, Ipus J J, Law J Y, Moreno-Ramírez L M and Conde A 2018 *Prog. Mater. Sci.* **93** 112
- [3] Shen B G, Sun J R, Hu F X, Zhang H W and Cheng Z H 2009 *Adv. Mater.* **21** 4545
- [4] Lee J S 2004 *Phys. Stat. Sol. (b)* **241** 1765
- [5] Phan M H and Yu S C 2007 *J. Magn. Magn. Mater.* **308** 325
- [6] Hcini S, Boudard M, Zemni S and Oumezzine M 2014 *Ceram. Int.* **40** 16041
- [7] Wali M, Skini R, Khelifi M, Dhahri E and Hlil E K 2015 *Dalton Trans.* **44** 12796

- [8] Yadav P A, Deshmukh A V, Adhi K P, Kale B B, Basavaiah N and Patil S I 2013 *J. Magn. Magn. Mater.* **328** 86
- [9] Deshmukh A V, Patil S I, Bhagat S M, Sagdeo P R, Choudhary R J and Phase D M 2009 *J. Phys. D: Appl. Phys.* **42** 185410
- [10] Dhahri I, Ellouze M, Mnasri T, Hlil E K and Jontania R B 2020 *J. Mater. Sci.: Mater. Electron.* **31** 12493
- [11] Ezaami A, Sellami-Jmal E, Cheikhrouhou-Koubaa W, Cheikhrouhou A and Hlil E K 2017 *J. Phys. Chem. Solids* **109** 109
- [12] Amaral J S, Das S and Amaral V S 2011 in J C M Pirajá (ed) *The mean-field theory in the study of ferromagnets and the magnetocaloric effect, thermodynamics-systems in equilibrium and non-equilibrium* (InTech) 173
- [13] Hamad M A 2014 *Phase Transit.* **87** 460
- [14] Hamad M A 2012 *Phase Transit.* **85** 106
- [15] Franco V, Blázquez J S and Conde A 2006 *Appl. Phys. Lett.* **89** 222512
- [16] Cowley R A 1980 *Adv. Phys.* **29** 1
- [17] Alzahrani B, Hsini M, Hsini S, Dhahri A and Bouazizi M L 2020 *Appl. Phys. A* **126** 1
- [18] Hsini M, Hcini S and Zemni S 2018 *J. Magn. Magn. Mater.* **466** 368
- [19] Krumhansl J A 1992 *Solid State Commun.* **84** 251
- [20] Amaral J S, Reis M S, Amaral V S, Mendonça T M, Araújo J P, Sáb M A *et al* 2005 *J. Magn. Magn. Mater.* **290** 686
- [21] Amaral V S and Amaral J S 2004 *J. Magn. Magn. Mater.* **272** 2104
- [22] Bourouina M, Krichene A, Chniba Boudjada N, Khitouni M and Boujelben W 2017 *Ceram. Int.* **43** 8139
- [23] Hsini M, Hcini S and Zemni S 2019 *Eur. Phys. J. Plus* **134** 588
- [24] Cardy J 1996 (eds) *Scaling and renormalization in statistical physics* (Cambridge University Press)
- [25] Dong Q Y, Zhang H W, Shen J L, Sun J R and Shen B G 2007 *J. Magn. Magn. Mater.* **319** 56
- [26] Gschneidner K A and Pecharsky V K Jr 2000 *Annu. Rev. Mater. Sci.* **30** 387
- [27] Rostamnejadi A, Venkatesan M, Kameli P, Salamati H and Coey J M D 2011 *J. Magn. Magn. Mater.* **323** 2214
- [28] Noumi M, Marouani Y, Dhahri R, Dhahri E, Hlil E K and Costa B F O 2021 *J. Alloys Compd.* **866** 157541
- [29] Banerjee B K 1964 *Phys. Lett.* **12** 16
- [30] Dong Q Y, Zhang H W, Sun J R, Shen B G and Franco V 2008 *J. Appl. Phys.* **103** 116101
- [31] Makni-Chakroun J, Omrani H, Cheikhrouhou-Koubaa W, Koubaa M and Cheikhrouhou A 2016 *J. Supercond. Nov. Magn.* **29** 1681
- [32] Ezaami A, Sellami-Jmal E, Cheikhrouhou-Koubaa W, Koubaa M and Cheikhrouhou A 2017 *J. Supercond. Nov. Magn.* **30** 911
- [33] Datta S, Guha S, Panda S K and Kar M 2020 *Phys. Stat. Sol. (b)* **257** 2000123
- [34] Hamad M A 2013 *J. Supercond. Nov. Magn.* **26** 2981
- [35] Zemni S, Baazaoui M, Dhahri Ja Vincent H and Oumezzine M 2009 *Mater. Lett.* **63** 489
- [36] Kallel N, Kallel S, Hagaza A and Oumezzine M 2009 *Phys. B: Condens. Matter* **404** 285
- [37] Zhang X X, Wen G H, Wang F W, Wang W H, Yu C H and Wu G H 2000 *Appl. Phys. Lett.* **77** 3072